

Spectral Color Reproduction of Paintings

Roy S. Berns, Lawrence A. Taplin, Philipp Urban, Yonghui Zhao; Munsell Color Science Laboratory, Chester F. Carlson Center for Imaging Science, Rochester Institute of Technology, Rochester, New York

Abstract

A spectral-based imaging system was constructed consisting of a two-sequential-absorption-filter-CFA digital camera and a seven-color inkjet printer and used to image and print a post-impressionist style painting such that matches were generated for CIE Illuminants D65 and A. Camera calibration was learning based using the Matrix R method. Rendered images for both illuminants were inputted to a color separation algorithm. First, conventional colorimetric gamut mapping was performed for the designated primary illuminant. Second, each pixel was transformed into a metameric printer gamut, that is, all possible ink combinations matching the primary illuminant. The ink combination with the smallest color difference for the secondary illuminant was selected as the color separation. Prints were prepared for each combination of primary and secondary illuminant and repeated for both CIE standard observers. The method was successful within limits of camera and printer spectral accuracy, ink design, and illuminant and observer metamerism.

Introduction

Reproducing the appearance of paintings in print is a common occurrence. In most museums, visual editing is an integral part of the workflow [1]. The amount of visual adjustment and the number of iterations required to achieve acceptability depends principally on the spectral properties of the artwork, the spectral sensitivities and color management of the camera, differences between the actual and assumed viewing illuminants, differences in size between the original and reproduction, the spectral properties of the printing materials and color management, and the matching objective (colorimetric, preferred, etc.). If the painting and print have the same size and matching is desired for multiple conditions, spectral reproduction becomes the matching objective. This objective has been achieved in the past using a multi-spectral camera and spectral printing models [2-5]. The limiting factor was the extreme computational load in generating color separations because, in essence, instrumental-based color matching using non-linear constrained optimization was performed at each pixel.

During the last years, there have been significant advances in spectral imaging of artwork [6], spectral processing [7-9], and spectral printing [10]. (These references are exemplars and not a definitive list.) Although these advances overcome the processing limitations of past research, spectral reproduction of artwork is still limited by metamerism, a result of printing inks' inability to span the spectral properties of artist materials. Thus, it was of interest to evaluate spectral color reproduction of a painting with a focus on metamerism.

Experimental

The general methodology is shown in Figure 1. A painting is imaged using a multi-spectral camera. Following spectral and spatial processing (denoising and sharpening), two CIELAB images are rendered for a standard observer and for primary and secondary illuminants. The coordinates for the primary illuminant are mapped within the printer's color gamut. For each

pixel, all ink combinations and their amounts are calculated yielding a metameric ensemble of spectra (metameric mismatch gamut for the secondary illuminant). This is possible when the number of inks exceed three. For each metamer, a color difference is calculated for the secondary illuminant. The ink combination leading to the smallest difference is selected.

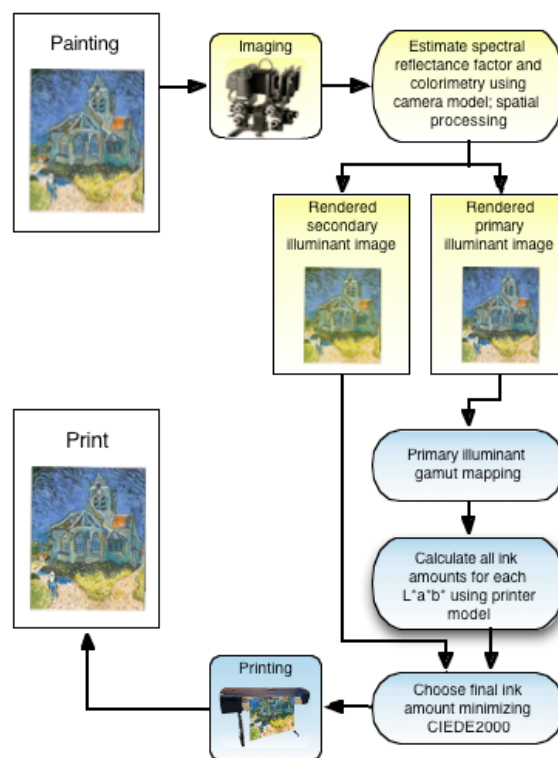


Figure 1. Experimental workflow. Yellow indicates imaging system and blue indicates printing system.

Painting

A set of artist acrylics were defined that reasonably spanned the spectral gamut of artist pigments [11]. These were used to make a painting in the style of Vincent van Gogh's Church at Auvers, shown in Figure 2.

Imaging system

A 22-megapixel Sinar digital camera system was modified as described by Berns [12], resulting in a six-channel multi-spectral camera. Lighting consisted of two tungsten-halogen Elinchrom Scanlite Digital 1000 sources affixed with Chimera diffusers. Lee #201 bluish gelatin filters were placed between the lamps and diffusers to achieve more spectrally uniform lighting (CCT = ~5400 K). Each light illuminated the object plane at 45° from the normal. Images were collected of a gray surface for flat fielding, a GretagMacbeth ColorChecker DC (CCDC) and a custom artist material target for calibration, and the painting.

A learning-based technique, known as the Matrix R method, was used to estimate spectral reflectance [13]. This method optimizes colorimetric and spectral accuracy simultaneously. Accordingly, transformations were derived for illuminants D65 and A and for both the 1931 and 1964 standard observers. Thus, four 16-bit CIELAB images were rendered. Sharpening was performed on the L* plane and noise was reduced on the a* and b* planes.

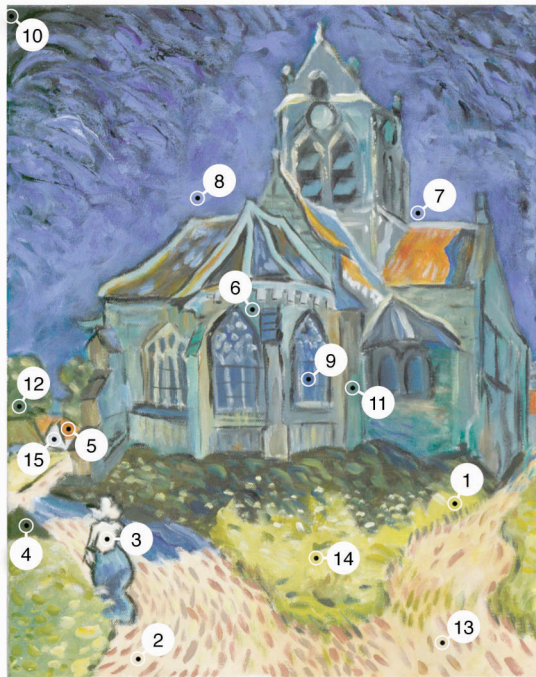


Figure 2. Auvers, Bernard Lehmans (16" x 20") 2007: rendered for D65 and the 1931 standard observer. Measurement locations notated.

Printing system

An HP Z3100 Photo inkjet printer was controlled by an Onyx Production House RIP 7.0. Of its 12 inks, only cyan, magenta, yellow, black, red, green, and blue were used. To reduce fluorescence in the final prints, a paper without optical whitener was used, Felix Schoeller (H74261) 270g/m². A calibration target of 7725 patches spanning the printer's spectral gamut and constrained to the paper's ink limits was printed and measured using an X-Rite i1iSis. The ink gamut was divided into four-ink sub-gamuts [2] and the cellular extension of the Yule-Nielsen Spectral Neugebauer equations was used to characterize each spectral sub-gamut in similar fashion to Chen [14].

The separation method combined spectral gamut mapping as well as model inversion in one single step. The basis of the separation is the spectral gamut-mapping framework described in detail in another CGIV 2008 paper [15]. The separation method compensated for both color discrimination and printing quantization artifacts. Using a traditional gamut mapping (chroma compression while preserving hue and lightness) within a hue-linearized [16] CIELAB color space for the primary illuminant, the CIELAB image was transformed into a metameric printer gamut. A 3D histogram was created for this image and for each sub-model the colorant space was sampled in 1% steps resulting in ~100 million different ink combinations. For the 20 sub-models a total of 2 billion colors were transformed by the forward model for the primary illuminant and tested using the 3D histogram for matching pixel-CIELAB

values of the already gamut-mapped image. For each ink combination matching a CIELAB pixel value for the primary illuminant, the corresponding CIELAB value for the second illuminant was calculated using the forward printer model and compared with the corresponding pixel CIELAB value for the second illuminant using ΔE_{00} . The ink combination with the smallest difference was used for the separation. The whole separation process required ~5 min for a 22-megapixel image on an Intel Q6600 quad-core processor using a performance optimized C++ implementation.

Results and Discussion

The spectral reflectance factors of fifteen positions, selected as representative colors, were measured using an X-Rite i1 on the painting and each print. The metameric mismatch gamuts for illuminant A (secondary illuminant) are plotted in Figure 3 for seven of the colors that did not overlap in the a*-b* projection. For some colors (e.g., blue and greenish yellow), the color of the painting was not within the mismatch gamut; thus it was not possible to produce a reproduction matching the painting except under a single reference condition. The spectral properties of the printer did not span the acrylic paints, in particular, ultramarine blue, the dominant paint used in the sky. This is shown in Figure 4 (position 8); the prints had different spectral characteristics than the painting. Although the printer's blue ink has a long wavelength reflectance tail, it did not coincide with ultramarine and the spectral differences beyond 600 nm are striking. Another example is the greenish yellow used between the split in the road (position 14). Hansa yellow medium, with a transition wavelength above 500 nm, was redder than the printer yellow, having a transition wavelength near 480 nm. Consequently, the print was metameric. An example of good performance is shown in Figure 6 for a grayish green color (position 6).

For each measurement position, the print spectra exhibited similar shape with appreciable variation. The color separation algorithm resulted in the same set of inks for each color, but a range of ink amounts. This was caused by changes in the primary and secondary illuminants, changes in the observer, and measurement uncertainty caused by positioning the spectrophotometer.

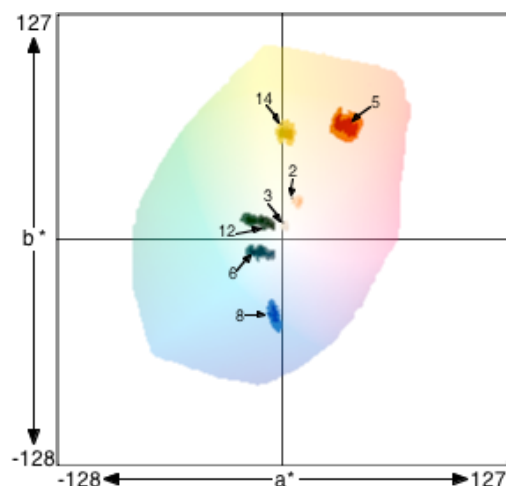


Figure 3. Metameric mismatch gamuts for seven positions on the painting (marked by arrow tips): illuminant A and the 1931 standard observer. The printer's gamut boundary is shown and the inner colored regions indicate where a match of CIEDE2000 < 2.0 is possible and the dark regions in their centers < 1.0 for the colors constrained to match under illuminant D65.

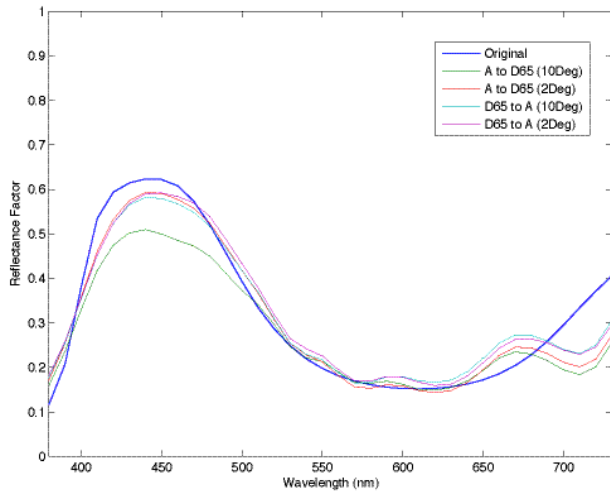


Figure 4. Spectral reflectance factor at measurement position 8 for painting (original) containing appreciable ultramarine blue and four prints.

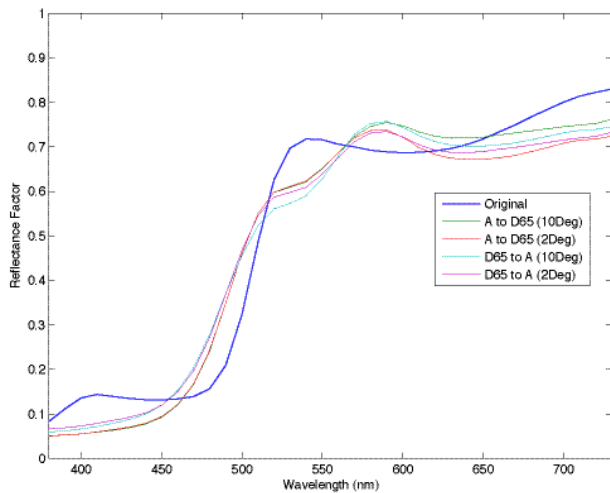


Figure 5. Spectral reflectance factor at measurement position 14 for painting (original) containing appreciable hansa yellow medium and four prints.

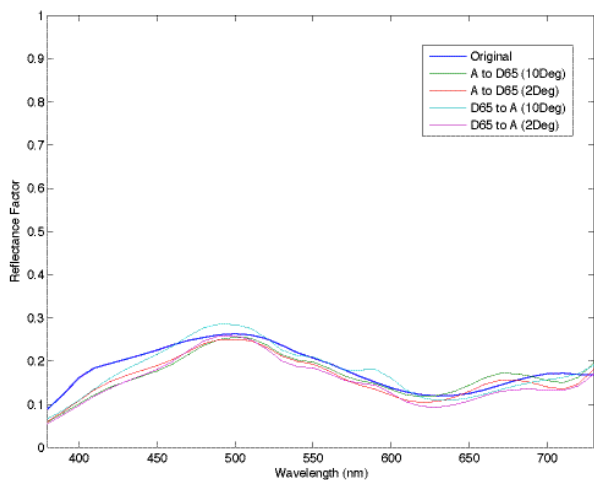


Figure 6. Spectral reflectance factor at measurement position 6 for painting (original) containing appreciable phthalocyanine green and four prints.

A number of comparisons were made in order to evaluate color accuracy for each imaging system and the end-to-end performance, the results summarized in Tables I-V. Comparisons were limited to the 15 measurement positions.

Printer Model Accuracy

The first analysis compared the predicted and measured print spectra, testing printer model accuracy (Table I). Since this is a non-metameric analysis, the specific viewing, primary, and secondary illuminants had a minimal effect. Accuracy was quite good with median and average CIEDE2000 values of two or less. Position 2 had the larger errors, perhaps due to measurement position error.

Table I – Printer Model Predicted vs Measured Print

Viewing Conditions	Illuminant D65				Illuminant A				
	2°		10°		2°		10°		
Print Pri. Ill.	D65	A	D65	A	D65	A	D65	A	
Print Sec. Ill.	A	D65	A	D65	A	D65	A	D65	
Measurement Location	1	1.0	1.8	1.4	1.7	1.0	1.7	1.5	1.7
	2	3.5	2.8	4.1	2.5	2.6	2.3	2.4	2.1
	3	2.9	1.5	2.7	2.6	2.0	1.1	1.1	1.9
	4	0.8	0.8	1.7	1.3	1.0	0.8	1.4	1.4
	5	1.2	1.3	3.3	1.4	1.3	1.8	2.2	1.7
	6	2.0	0.6	2.5	1.7	1.6	0.9	2.5	1.3
	7	2.1	1.4	2.1	1.2	1.8	1.3	2.0	1.2
	8	2.1	1.3	0.9	1.1	1.9	1.6	0.9	1.1
	9	0.8	2.5	3.7	0.8	1.0	2.6	3.1	0.9
	10	1.5	1.1	1.7	1.5	1.6	1.1	1.7	1.4
	11	1.0	1.3	1.1	0.9	0.7	1.1	1.0	1.0
	12	1.0	1.5	3.3	1.5	1.1	1.5	2.9	1.8
	13	2.0	1.3	0.6	1.1	1.4	1.1	0.4	0.8
	14	0.9	0.5	0.5	1.0	1.0	0.3	0.4	0.6
	15	1.3	1.0	0.4	0.9	0.7	0.6	1.0	0.9
Mean	1.6	1.4	2.0	1.4	1.4	1.3	1.6	1.3	
Median	1.3	1.3	1.7	1.3	1.3	1.1	1.5	1.3	

Camera Accuracy

The second analysis was the camera accuracy independent from the printing system (Table II). For D65 and the 1931 observer, median performance was typical when comparing with contact spectrophotometry [12, 13]. However, the performance for dark colors (positions 4 and 10) was poor. One source of error was image noise. Despite tuning the camera-taking source to have an approximately spectrally flat output across the visible spectrum, there was still the expected reduction in output at short wavelengths and since a CFA sensor was used, the dynamic range for the blue channel was smaller than the other channels. The second source of error was differences in gloss between the calibration target and the painting and differences in lighting geometry between the spectrophotometer and the imaging system. These differences have a greater affect on dark colors. The third source of error was the transformation matrix; in essence, a single transformation is mapping camera to spectral spaces. This transformation is a compromise in performance over the dynamic ranges of both spaces, particularly because the transformation is nearly linear. Another interesting result was comparing the illuminant A performance for the two observers; the 1964 observer had color differences twice the magnitude of the 1931 observer. Apparently, differences in the spectral

properties between the calibration targets and the painting had a more pronounced effect for this illuminant/observer pair.

Table II – Original vs Spectral Based Camera Estimate

Viewing Conditions		Illuminant D65		Illuminant A	
		2°		10°	
		2°	10°	2°	10°
Measurement Location	1	1.4	1.7	1.3	2.3
	2	0.9	1.0	1.0	3.3
	3	1.0	1.4	0.7	5.3
	4	9.5	10.3	3.7	5.0
	5	3.4	3.3	2.1	2.1
	6	2.5	2.2	2.1	3.7
	7	1.0	0.7	0.9	2.7
	8	0.9	0.9	1.0	2.7
	9	1.7	0.8	2.1	1.3
	10	10.9	11.9	4.2	5.9
	11	3.0	2.7	2.8	3.7
	12	2.9	2.9	2.5	3.1
	13	1.1	1.1	1.1	3.3
	14	1.1	1.5	0.6	2.1
	15	1.5	1.6	1.6	7.4
Mean		2.8	2.9	1.8	3.6
Median		1.5	1.6	1.6	3.3

Gamut Mapping

The third comparison was evaluating the predicted print spectra with the spectra predicted by the camera (Table III). This is an indicator of color gamut limitations for cases where the viewing and primary illuminants are matched. The median values are all below one; thus, the extent of color gamut mapping was negligible. Comparing the order of primary and secondary illuminants (e.g., D65/A vs. A/D65) indicates the degree of metamerism that results from the printing ink spectra not spanning the artist pigment spectra. For many positions, there was an increase in color difference when the secondary and viewing illuminants were unmatched. Similar to the camera evaluation, the choice of observer affected performance.

Table III – Camera Estimate vs Print Predicted

Viewing Conditions		Illuminant D65				Illuminant A			
		2°		10°		2°		10°	
Print Pri. Ill.		D65	A	D65	A	D65	A	D65	A
Print Sec. Ill.		A	D65	A	D65	A	D65	A	D65
Mean		0.8	1.4	1.0	2.9	1.3	0.8	2.6	0.7
Max		2.9	5.8	3.4	6.6	2.7	1.5	5.3	1.7
Median		0.6	0.7	0.8	2.2	1.1	0.6	2.1	0.6

Printing System Accuracy

The fourth comparison was evaluating the actual print spectra with the spectra predicted by the camera (Table IV). This is a measure of printer accuracy. One expects actual printing to diverge from virtual printing, i.e., predicted print spectra. For these samples, overall median performance decreased by a factor of two. Changes in printer characteristics and lack of model accuracy were the two main contributors. Even so, the level of performance achieved was reasonable. Again, the choice of observer affected measured performance.

Table IV – Camera Estimate vs Measured Prints

Viewing Conditions		Illuminant D65				Illuminant A			
		2°		10°		2°		10°	
Print Pri. Ill.		D65	A	D65	A	D65	A	D65	A
Print Sec. Ill.		A	D65	A	D65	A	D65	A	D65
Measurement Location	1	1.1	2.1	1.5	2.2	1.9	1.7	3.0	1.8
	2	3.7	2.6	4.2	1.7	3.6	2.9	5.9	2.8
	3	3.3	1.6	2.8	2.8	3.6	2.1	6.1	3.0
	4	1.8	4.4	1.0	4.8	3.3	0.8	4.9	1.0
	5	1.7	0.8	3.3	1.5	2.4	1.9	2.8	1.8
	6	1.6	1.0	2.6	3.7	1.1	0.8	3.3	1.3
	7	2.1	1.7	1.9	2.0	1.4	1.1	2.8	1.0
	8	2.1	1.8	0.8	1.7	1.4	1.1	1.9	0.8
	9	0.6	1.5	3.3	2.5	1.2	2.6	3.8	0.8
	10	2.4	6.6	3.0	7.8	3.9	2.0	3.4	2.1
	11	0.8	1.5	1.7	2.5	0.5	0.8	2.5	0.3
	12	1.8	2.5	3.2	2.4	1.7	1.9	3.8	1.8
	13	2.1	1.2	0.7	2.1	2.2	1.5	3.0	1.3
	14	1.1	0.9	0.7	1.5	2.2	0.6	2.5	0.8
	15	1.6	1.6	1.1	6.3	1.7	2.0	4.8	2.4
Mean		1.8	2.1	2.1	3.0	2.1	1.6	3.6	1.5
Median		1.8	1.6	1.9	2.4	1.9	1.7	3.3	1.3

End-to-end performance

The fifth comparison was an end-to-end evaluation, comparing the painting with printed reproductions (Table V). The uncertainties from measurement, imaging, and printing propagate through the system. This corresponds to the original-to-camera and print-predicted-to-print color differences. If it is assumed that color differences represent independent uncertainties, then the total uncertainty is the root-sum-square of color differences [17]. The estimated uncertainty and the actual performance were equivalent; thus the error propagation followed theoretical expectations and characterizing individual uncertainties can be used to estimate end-to-end performance. We see that the camera errors, as the first system component, have a large impact on the total uncertainty. The dark samples, positions 4 and 10, had large camera errors that remained in the prints. If these are interpreted as outliers, then the median values are a better indicator of total performance since the majority of the painting is lighter. These values were excellent, particularly because contact measurements of paintings introduce considerable uncertainty because of a non-uniform surface, both in color and topography (impasto).

Table V – Original Painting vs Measured Prints

Viewing Conditions		Illuminant D65				Illuminant A			
		2°		10°		2°		10°	
Print Pri. Ill.		D65	A	D65	A	D65	A	D65	A
Print Sec. Ill.		A	D65	A	D65	A	D65	A	D65
Measurement Location	1	2.0	3.4	1.7	3.9	2.3	2.9	2.2	3.4
	2	4.0	2.8	4.6	2.5	3.9	3.2	4.0	2.9
	3	4.0	2.2	3.9	3.9	3.7	2.3	3.5	4.6
	4	7.8	6.0	10.0	6.9	5.9	4.1	7.6	5.2
	5	2.6	3.5	0.3	3.3	1.7	1.5	0.8	0.9
	6	3.9	3.1	2.2	4.8	3.1	2.4	1.4	4.1
	7	1.5	1.4	1.5	2.7	1.0	1.1	1.7	2.9
	8	2.6	2.0	1.6	2.3	2.3	1.1	2.4	2.9
	9	2.0	3.0	4.0	2.2	2.8	4.0	3.8	2.1
	10	9.3	5.8	10.2	6.4	6.7	5.0	7.3	6.0
	11	3.4	3.3	1.6	4.2	3.0	2.5	1.8	4.0
	12	1.5	1.5	3.2	2.0	2.8	1.4	2.9	1.6
	13	2.3	1.8	1.5	3.1	2.5	2.1	1.7	3.1
	14	1.6	0.5	1.7	1.3	2.4	0.8	2.7	1.7
	15	2.1	2.6	2.6	7.9	1.8	2.8	2.7	9.0
Mean	3.4	2.9	3.4	3.8	3.1	2.5	3.1	3.6	
Median	2.6	2.8	2.2	3.3	2.8	2.4	2.7	3.1	

Observer Metamerism

In this evaluation, the influence of the choice of standard observer was evaluated. There was a trend where color differences including the degree of metamerism (unmatched viewing and primary illuminants) were larger for the 1964 observer. The colorimetry for the sky was sensitive to the choice of observer. The tristimulus values for measurement position 8 were calculated for both observers and D65. These values were transformed to sRGB and rendered, shown in Figure 7. It is observed that the colors change quite dramatically. This sensitivity was observed when comparing the various prints with the painting under tungsten and fluorescent daylight. The choice of observer changed to relative appearance of the blue sky in the prints compared with the painting from reddish to greenish for the 1931 and 1964 observer, respectively.

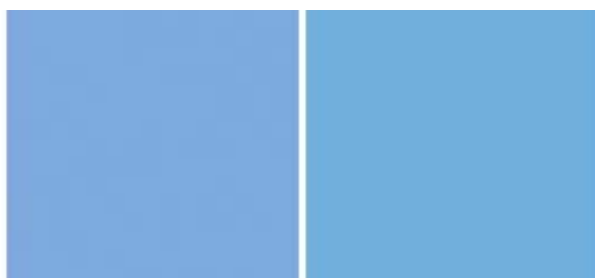


Figure 7. Position 8 rendered for the 1931 (left) and 1964 (right) standard observers and D65. Rendering used a single transformation.

Conclusions

An end-to-end spectral-based color-reproduction system was constructed and evaluated. The system used a multi-spectral digital camera and a seven-ink inkjet printer. Both systems were modeled spectrally, each achieving reasonable performance. The total color accuracy varied with the choice of standard illuminant and observer with mean and median CIEDE2000 values above

and below three, respectively. The analysis also demonstrated the difficulty in reproducing artist pigments with inkjet inks.

References

- [1] RS Berns, FR Frey, MR Rosen, EP Smoyer, LA Taplin. Direct Digital Capture of Cultural Heritage: Benchmarking American Museum Practices and defining Future Needs. Rochester, NY: RIT. (2005).
- [2] DY Tzeng, RS Berns. Spectral-based six-color separation minimizing metamerism. Proc. IS&T/SID Eighth Color Imaging Conference, 342-347 (2000).
- [3] FH Imai, MR Rosen, DR Wyble, RS Berns, DY Tzeng. Spectral reproduction from scene to hardcopy I: input and putput. Proc. SPIE 4306B 346-357 (2001).
- [4] LA Taplin, RS Berns. Spectral color reproduction based on a six-color inkjet output system. Proc. IS&T/SID Ninth Color Imaging Conference, 209-213 (2001).
- [5] FH Imai, DR Wyble, RS Berns, DY Tzeng. A feasibility study of spectral color reproduction. J. Imag. Sci. Tech. 47, 543-553 (2003).
- [6] C Fischer, I Kakoulli. Multispectral and hyperspectral imaging technologies in conservation: current research and potential applications. Reviews in Conservation. 7, 3-16 (2005).
- [7] MR Rosen, FH Imai, X Jiang, N Ohta. Spectral reproduction from scene to hardcopy II: Image processing. Proc. SPIE 4300, 33-41 (2001).
- [8] MW Derhak, MR Rosen. Spectral colorimetry using LabPQR – an interim connection space. J. Imaging Sci. Technol, 50, 53-63 (2006).
- [9] S Tsutsumi, MR Rosen, RS Berns. Spectral color reproduction using an interim connection space-based lookup table. Proc. IS&T/SID Fifteenth Color Imaging Conference, 184-189 (2007).
- [10] P Urban, MR Rosen, RS Berns. Accelerating spectral-based color separation within the Neugebauer subspace. J. Electronic Imaging, 16(4), 043014 (2007).
- [11] M Mohammadi, M.Nezamabadi, RS Berns, LA Taplin. Spectral imaging target development based on hierarchical cluster analysis, Proc. IS&T/SID Twelfth Color Imaging Conference, 59-64 (2004).
- [12] RS Berns, LA Taplin. Practical Spectral imaging Using a Color-Filter Array Digital Camera, MCSL Technical Report, July 2006. www.art-si.org
- [13] Y Zhao, RS Berns. Image-based spectral reflectance reconstruction using the Matrix R method, Color Res. Appl., 32, 343-351 (2007).
- [14] Y Chen, RS Berns, LA Taplin. Six color printer characterization using an optimized cellular Yule-Nielsen spectral Neugebauer model, J. Imag. Sci. Tech. 48, 519-528 (2004).
- [15] P Urban, MR Rosen, RS Berns. Spectral gamut mapping framework based on human color vision. Proc. CGIV2008/MCS'08, see this proceedings (2008).
- [16] PC Hung, RS Berns. Determination of constant hue loci for a CRT gamut and their predictions using color appearance spaces. Color Res. Appl. 20, 285-295 (1995).
- [17] EA Early, ME Nadal. Uncertainty analysis for the NIST 0:45 reflectometer. Color Res. Appl. 33, 100-107 (2008).

Acknowledgments

This research was supported by the Andrew W. Mellon foundation and the Museum of Modern Art, New York. Equipment and software donations were received from Hewlett Packard and Onyx Graphics, respectively.

Author Biographies

Roy S. Berns holds the Richard S. Hunter Professorship in Color Science, Appearance, and Technology and is the Coordinator of the Color Science graduate programs at RIT. He leads a research group that includes the co-authors in the spectral and geometric imaging, archiving, and reproduction of cultural heritage. Lawrence A. Taplin is a Color Scientist, Philipp Urban is a Visiting Researcher, and Yonghui Zhao is a recent graduate from RIT's Imaging Science Ph.D. program.